The Blazar Sequence and the Cosmic Gamma-Ray Background Radiation

Yoshiyuki Inoue[1], Tomonori Totani[1] and Takuro Narumoto[1]

[1] Department of Astronomy, Kyoto University, Kitashirakawa, Sakyo-ku, Kyoto 606-8502, Japan
E-mail(YI): yinoue@kusastro.kyoto-u.ac.jp

Abstract

We present a new model of the blazar gamma-ray luminosity function (GLF) based on the EGRET blazar data, and study the contribution to extragalactic gamma-ray background (EGRB) radiation, taking into account the unified sequence of blazar spectral energy distribution (SED). This enables us to predict the EGRB spectrum in more realistic way than previous studies. We construct a model spectrum of EGRB by summing up the blazar EGRB component and another non-blazar AGN component, which is dominant in the cosmic X-ray background radiation. The non-blazar component has a nonthermal steep tail in EGRB spectrum, and it is dominant against the blazar component up to ~ 100 MeV. The model EGRB flux and spectrum are in nice agreement with the observed data from X-ray to 1 GeV band. These results indicate that AGNs including blazars are the major contributor to the high energy background radiation from X-ray to gamma-ray bands. Quantitative predictions for GLAST are also made.

Key words: workshop: proceedings — LaTeX2.09: style file — instructions

1. introduction

The origin of the extragalactic diffuse gamma-ray background (EGRB) has been argued in astrophysics for a long time. The EGRB spectrum was first discovered by the *SAS 2* satellite (Fichtel, Simpson, & Thompson 1978; Thompson & Fichtel 1982). Subsequently, the EGRB spectrum was confirmed up to an energy ~ 50 GeV by EGRET on board the Compton Gamma Ray Observatory. The EGRB flux is about 1×10^{-5} photons cm^{-2} s^{-1} sr^{-1} above 100 MeV and the spectrum is approximately a power law with a photon index of -2 in a wide range of $\sim$30 MeV – 100 GeV (Sreekumar et al. 1998; Strong, Moskalenko, & Reimer 2004a). It should be noted that, however, the EGRB measurement is strongly dependent on the modeling of foreground emission, which is dominated by the diffuse Galactic emission from cosmic-ray interactions in the Galactic disk region and must carefully be subtracted from the total background flux (Keshet, Waxman, & Loeb 2004; Strong, Moskalenko, & Reimer 2004b; Kamae, Abe, & Koi 2005).

Although several sources of gamma-rays (e.g., clusters of galaxies or dark matter annihilation) have been proposed as a significant contributor to EGRB [see, e.g., Narumoto & Totani (2006) and references therein], active galactic nuclei (AGNs) of the blazar class have been thought as the primary candidate for the origin of EGRB, since almost all of the extragalactic gamma-ray sources detected by EGRET are blazars. The blazar contribution to EGRB have been estimated by a number of papers (Padovani et al. 1993; Stecker, Salamon, & Malkan 1993; Salamon & Stecker 1994; Chiang et al. 1995; Stecker & Salamon 1996; Chiang & Mukherjee 1998; Mücke & Pohl 2000; Narumoto & Totani 2006; Giommi et al. 2006; Dermer 2007; Kneiske & Mannheim 2008).

Stecker & Salamon (1996) estimated that 100% of the EGRB radiation can be explained by blazars. However, their model was constructed based on the blazar luminosity function in radio bands, without comparison with the gamma-ray flux and redshift distributions of the EGRET blazars. Therefore it was not certain whether their model was statistically consistent with the EGRET blazar data. Chiang & Mukherjee (1998) found that only 20–40% of EGRB can be accounted for by blazars, taking into account the EGRET blazar data and assuming pure luminosity evolution for blazar LF. Narumoto & Totani (2006, hereafter NT06) extended this kind of analysis by introducing a luminosity-dependent density evolution (LDDE) of blazar GLF, which is motivated from the evolution of X-ray luminosity function (XLF) of AGNs. NT06 found that the LDDE model fits to the EGRET blazar data better than PLE models, and also confirmed that only 25–50% of EGRB can be explained by blazars. In most of these studies, however, it was assumed that the spectral energy distribution (SED) of blazars is a simple power-law, or a broken power-law with no dependence on the blazar luminosity.

Blazar SED has been theoretically and observationally studied in detail(Ghisellini & Tavecchio 2008, and

references therein). Blazar emission is widely believed to be the sum of the synchrotron and inverse Compton emission components produced by the same nonthermal electron population accelerated in relativistic jets. Multi-wavelength observational studies from radio to γ-ray bands have indicated an interesting feature in blazar SEDs; the synchrotron and Compton peak photon energies decrease as the bolometric luminosity increases (Fossati et al. 1997, 1998; Donato et al. 2001, Ghisellini & Tavecchio 2008; but see also Padovani et al. 2007). This is often called as the blazar SED sequence.

Here we predict the EGRB flux and spectrum from blazars, by constructing a blazar GLF model that is consistent with the flux and redshift distributions of the EGRET blazars, based on the LDDE model and the blazar SED sequence. By introducing the blazar SED sequence, we can make a reasonable prediction of the EGRB spectrum for the first time. Recently, Inoue, Totani, & Ueda (2008) has showed that the EGRB in the MeV band can naturally be explained by normal (i.e., non-blazar) AGNs that are the origin of the cosmic X-ray background. This MeV background component extends to ~ 100 MeV by the Comptonization photons produced by nonthermal electrons in hot coronae. Therefore, it should also contribute to the EGRB at ≤ 1 GeV. We will also make quantitative predictions for the Gamma-Ray Large Area Space Telescope (GLAST) that has successfully been launched on June 11th, 2008. Throughout this paper, we adopt the standard cosmological parameters of $(h, \Omega_M, \Omega_\Lambda)$=(0.7,0.3,0.7).

2. The Blazar SED Sequence

Fossati et al. (1997, 1998) and Donato et al. (2001, hereafter D01) constructed empirical blazar SED models based on fittings to observed SEDs from radio to γ-ray bands. These models are composed of the two components (synchrotron and Inverse Compton), and each of the two is described by a linear curve at low photon energies and a parabolic curve at high energies.

Here we construct our own SED sequence model mainly based on the SED model of D01, because there is a mathmatical discontinuity in the original D01 model. In this model the two different mathematical fitting formulae are used below and above the luminosity $\nu L_\nu = 10^{43}$ erg s^{-1} at 5GHz, and the luminosity of the inverse-Compton component suddenly changes with a jump at this critical luminosity. Once the blazar luminosity is specified at a reference frequency, this empirical model gives the full blazar SED from radio to gamma-ray bands. In Fig.1 we show this empirical blazar SED sequence model in comparison with averaged observed SED data (Fossati et al. 1998; D01). We will calculate EGRB with this model of the blazar SED sequence.

3. The Model of Gamma-ray Luminosity Function of Blazars

3.1. Relating Jet Power and X-ray Luminosity of AGNs

The cosmological evolution of X-ray luminosity function of AGNs has been investigated intensively (Ueda et al. 2003 (hereafter U03); Hasinger, Miyaji, & Schmidt 2005 (hereafter H05); Gilli, Comastri, & Hasinger 2007). These studies revealed that AGN XLF is well described with the LDDE model, in which peak redshift of density evolution increases with AGN luminosity. Here we construct two models of blazar GLF based on the two XLFs derived by U03 (in hard X-ray band) and H05 (in soft X-ray band). It is natural to expect that power of blazar jet is correlated with the mass accretion rate to the central super massive black hole, which is also correlated with the X-ray luminosity from accretion disk. Therefore we simply assume that the bolometric luminosity of radiation from jet, P, is proportional to disk X-ray luminosity, L_X. It should be noted that L_X is *not* the observed X-ray luminosity of a blazar having a jet luminosity P. This treatment is observationally supported from the EGRET blazar data, because NT06 found a better agreement between the LDDE model and the data than PLE models, adopting this treatment.

3.2. Model Formulations

In this paper we describe the blazar GLF in terms of νL_ν luminosity at rest frame reference energy $\epsilon_{\rm ref,res} \equiv 100$ MeV. According to the assumption justified in the previous section, we simply relate the bolometric blazar luminosity P and X-ray luminosity by the parameter q, as $P = 10^q L_X$. Here, we define the disk luminosity L_X to be that in the rest frame 2–10 and 0.5–2 keV bands for the hard XLF (U03) and the soft XLF (H05), respectively. Thus, L_γ and L_X have been related through P.

The blazar GLF is then obtained from the AGN XLF,

$$\rho_\gamma(L_\gamma, z) = \kappa \frac{dL_X}{dL_\gamma} \rho_X(L_X, z), \quad (1)$$

where ρ_X and ρ_γ are the XLF and GLF, i.e., the comoving number densities of AGNs and blazars per unit X-ray and gamma-ray luminosity, respectively. The parameter κ is a normalization factor, representing the fraction of AGNs showing blazar activity. In our GLF model, we adopt the same form in U03 and H05 for ρ_X, as $\rho_X(L_X, z) = \rho_X(L_X, 0) f(L_X, z)$, where $\rho_X(L_X, 0)$ is the AGN XLF at present, which is characterized by the faint-end slope index γ_1, the bright-end slope index γ_2, and the break luminosity L_X^*, given as

$$\rho_X(L_X, 0) = \frac{A_X}{\ln(10) L_X} \left[\left(\frac{L_X}{L_X^*} \right)^{\gamma_1} + \left(\frac{L_X}{L_X^*} \right)^{\gamma_2} \right]^{-1} \quad (2)$$

and $f(L_X, z)$ is the density evolution function.

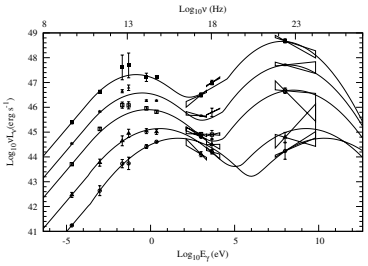

Fig. 1. The average SED of the blazars studied by Fossati et al. (1998), and D01. The each thin solid line represent the modified blazar spectra in this paper.

We set the minimum of the gamma-ray luminosity $L_{\gamma,\rm min}$=10^{43} erg s^{-1}, which is roughly corresponding to the lowest disk X-ray luminosity $L_X = 10^{41.5}$ erg s^{-1} set in U03 and H05, with typical values of the q parameter found in the likelihood analysis below.

4. Gamma-Ray Luminosity Function Determined by the EGRET Blazar Data

We use the maximum likelihood method to search for the best-fit model parameters of the blazar GLF to the distributions of the observed quantities of the EGRET blazars (gamma-ray flux and redshift). The analysis method and the data used are essentially the same as those in NT06.

In the first analysis, we take q as the only one free parameter for the U03 hard XLF and H05 soft XLF, with the XLF model parameters fixed at the values of U03 and H05. These are hereafter called as U03(q) and H05(q) fits, respectively. In the second analysis, we also take the faint-end slope index of XLF, γ_1, as another free parameter in addition to q. These are hereafter called as U03(q, γ_1) and H05(q, γ_1) fits, respectively. The best-fit values for these four fits are shown in Table.1. Figure 2 and Figure 3 show the redshift and luminosity distributions for the best-fit parameters with binned EGRET data. Quantitatively, the chance probabilities of getting the observed deviation estimated from the KS test are also shown in Table 1 and Table 2. Since the best KS test value is in the H05(q, γ_1) GLF model and H05 is the more recent XLF model, we basically discuss with H05(q, γ_1) GLF model below.

Table 1. Best-fit parameters for blazar GLF

	U03(q)	U03(q,γ_1)	H05(q)	H05(q,γ_1)
q	4.90	4.93	5.20	5.29
γ_1	0.86	1.06	0.87	1.26
κ	1.0×10^{-5}	7.6×10^{-6}	3.5×10^{-6}	1.5×10^{-6}

Table 2. KS test probability

	U03(q)	U03(q,γ_1)	H05(q)	H05(q,γ_1)
z	33.5%	25.4%	0.01%	29.3%
L_γ	47.6%	71.8%	1.3%	66.9%

5. The Gamma-Ray Background Spectrum

5.1. the EGRB Spectrum Calculation

We calculate the EGRB spectrum by integrating our blazar SED sequence model in the redshift and luminosity space, using the blazar GLF derived in §3. High energy photons ($>$ 20 GeV) from high redshift are absorbed by the interaction with the cosmic infrared background (CIB) radiation (Salamon & Stecker 1998; Totani & Takeuchi 2002; Kneiske et al. 2004), and $\tau_{\gamma\gamma}(z, \epsilon_\gamma)$ is the optical depth of the universe against this reaction, for a gamma-ray emitted from a source redshift z and received by an observer at $z = 0$ with a photon energy of ϵ_γ. In this paper, we adopted std model in Totani & Takeuchi 2002 for CIB model. Since these interaction creates e^+e^- pair, the created electrons would scatter cosmic microwave background (CMB) radiation (cascading emission) (Aharonian et al. 1994). We calculated the cascading emission as in Kneiske & Mannheim (2008).

5.2. The EGRB Spectrum by Blazars

Figure 4 shows the νF_ν EGRB spectrum predicted by the best-fit GLF model parameters obtained above. Here, we show the total EGRB flux as well as the contributions from different L_γ ranges. This EGRB spectrum is the primary spectrum directly from blazars, because in this calculation the effect of CIB absorption is included but the reprocessed emission by secondary electrons/positrons produced in IGM is not included. The data of *SMM* (Watanabe et al. 1999), COMPTEL (Kappadath et al. 1996) and EGRET (Strong et al. 2004a) are also shown. An important implication here is that the contribution from the so-called MeV blazars, which have their SED peaks at around MeV, is negligible for

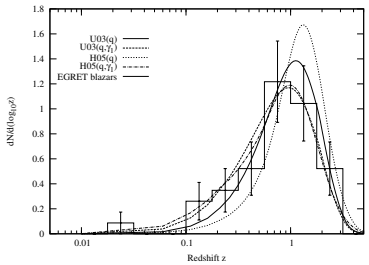

Fig. 2. Redshift distribution of the EGRET blazars. The histogram is the binned EGRET data. The solid, dashed, dotted, and dotted-dashed curves are the best-fit models for the U03(q), H05(q), U(q, γ_1), H05(q, γ_1) GLF model, respectively. The error bars are 1 σ Poisson error.

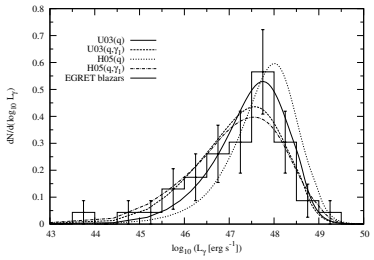

Fig. 3. Same as Fig.2, but for luminosity distribution of blazars of the EGRET blazars.

the MeV gamma-ray background, although such MeV blazars have been suspected as a possible origin of the MeV background. This is because MeV blazars have a large luminosity according to the blazar SED sequence, and the number density of such blazars is small in GLF.

5.3. EGRB from All AGNs and the Origin of EGRB

The total EGRB spectrum from blazars as well as non-blazar AGNs (gamma-rays from accretion disks) is shown in Figure 5. Here, the non-blazar component is the model constructed by Inoue et al. (2008), in which the EGRB in MeV range is explained by nonthermal electrons that is assumed to exist ubiquitously in hot coronae around AGN accretion disks. There is some discrepancy between the MeV EGRB data of *SMM* and COMPTEL, and the origin of this is not clear. Here we use two model parameter sets of $(\Gamma, \gamma_{\rm tr}) = (3.5, 4.4)$ and $(3.8, 4.4)$ in the Inoue et al.'s model, where Γ is the power-law index of nonthermal electron energy distribution and the $\gamma_{\rm tr}$ is the transition electron Lorentz factor above which the nonthermal component becomes dominant. These two parameter sets are chosen so that each of the two fits well to either of the SMM or COMPTEL data.

There is an excess of the EGRB data around GeV, compared with our model prediction. An interesting possibility is that such an excess is due to another component that is completely different from blazars, such as, dark matter annihilation (e.g., Oda, Totani, & Nagashima 2005). However, such GeV excess is also seen in the Galactic gamma-ray background spectrum (Pohl & Esposito 1998; Strong et al. 2004b; de Boer et al. 2005; Kamae, Abe, & Koi 2005), and Stecker, Hunter, & Kniffen (2008) have recently shown that these anomalies around GeV are likely caused by the systematic uncertainty in the calibration of the EGRET detector. They proposed the re-normalization factors for the EGRET data at the energy range from 30 MeV to 10 GeV, to make the EGRET data fit to the theoretically predicted galactic background spectrum. The cosmic X-ray and gamma-ray background spectrum with the EGRET data corrected by these factors is shown in Figure 5. Now the cosmic X-ray and gamma-ray background radiation are nicely explained by the emission from blazars and non-blazar AGNs in the entire range from X-ray to 10 GeV. Based on these results, we conclude that most of the EGRB flux can be explained by blazars and non-blazar AGNs, by GLFs that are consistent with the EGRET blazar data and AGN LF in X-ray band. Our prediction will soon be tested in much more detail by the GLAST data.

6. Predictions for the GLAST mission

Figure 6 shows the cumulative distribution of > 100 MeV photon flux of blazars. The four GLF models of U03(q), U03(q, γ_1), H05(q), and H05(q, γ_1), predict that about 480, 1040, 370, and 1560 blazars should be detected by GLAST, respectively, where we assumed the GLAST sensitivity to be $F_{\rm lim} = 2 \times 10^{-9}$ photons cm^{-2} s^{-1}. We find that the predicted fraction of resolved EGRB flux is $\sim 95\%$ against the total EGRB flux from all blazars

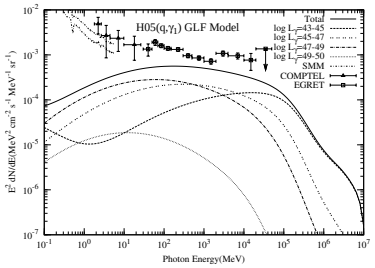

Fig. 4. Predicted spectrum of the cosmic background radiation in gamma-ray bands with H05(q, γ_1) GLF model. The data points of *SMM*(Watanabe et al. 1999), COMPTEL (Kappadath et al. 1996), EGRET (Strong et al. 2004a) experiments are also shown. The solid curves corresponds to the best-fit total background spectrum from blazars and non-blazars.

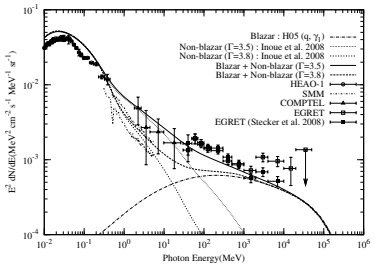

Fig. 5. Predicted spectrum of the cosmic background radiation in X-ray and gamma-ray bands based on our GLF model with H05(q, γ_1) GLF model. The data points of *HEAO-1* (Gruber et al. 1999), *SMM*, COMPTEL, EGRET experiments are also shown. The filled square data shows the correlated EGRET data using the Stecker et al. (2008) method. The solid curves corresponds to the background flux from blazar emission without the absorption effect. The dashed curves corresponds to that with the absorption effect. The dotted curves is the intergalactic cascading emission. The dotted-dashed lines is the total flux.

in the GLF model. Therefore, the EGRB from blazars should practically be resolved by GLAST. However, as seen in Fig. 5, there is a considerable contribution from non-blazar AGNs to the EGRB flux at 100 MeV, and this issue will be discussed below. Furthermore, resolvable fraction of total EGRB flux and of the hole blazar EGRB flux by blazars expected to be detected by GLAST is (37 %, 95 %) for the H05(q,γ_1) GLF model.

7. Conclusions

In this paper, we constructed a new model of the blazar gamma-ray luminosity function (GLF), taking into account the blazar SED sequence and the LDDE luminosity function evolution inferred from X-ray observations of AGNs. An implicit assumption here is that the jet activity of AGNs is associated with the accretion activity, and hence the blazar luminosity function has a similar evolution to that of X-ray AGNs. The GLF model parameters are constrained by fitting to the observed flux and redshift distribution of the EGRET blazars. By this model, for the first time, we can predict the spectrum of the extragalactic gamma-ray background (EGRB), rather than assuming a single power-law spectrum. The contribution from non-blazar AGNs to low energy EGRB is also considered, by using the model of Inoue et al. (2008) for the nonthermal emission from AGN accretion disks extending from MeV to higher energy band with a steep power-law.

The predicted EGRB flux and spectrum by the sum of blazars and non-blazar AGNs is in good agreement with the high energy background radiation data from X-ray to ~ 1 GeV, indicating that the EGRB below 1 GeV can mostly be explained by a combination of blazars and non-blazar AGNs. It should be noted that the contributions from blazars and non-blazar AGNs are comparable at 100 MeV. The previous studies about blazar GLF and EGRB concluded that at most 50% of EGRB can be explained when one constructs a GLF model that is consistent with the EGRET blazar data, and these studies considered the EGRB flux beyond the standard photon energy of EGRET catalog, i.e., 100 MeV. Therefore, previous studies and this work is nicely consistent with each other. At the photon energy range of > 1 GeV, the non-blazar component becomes negligible in the EGRB flux, and hence we predict that most of the EGRB flux should be accounted for by blazars. The EGRB data by Strong et al. (2004a) beyond 2 GeV are significantly higher than our model EGRB spectrum, and this may indicate the existence of another component. However, as argued by Stecker et al. (2008), there may be systematic error in the calibration of EGRET detector around GeV. If we correct the EGRET EGRB data by the factors proposed by Stecker et al. (2008), all the EGRB data are

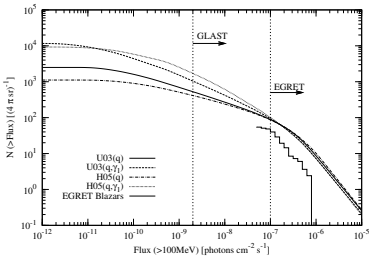

Fig. 6. log N - log F distribution of blazars. Each curve corresponds to U03(q), H05(q), U(q, γ_1), H05(q, γ_1) GLF model. The thin solid line shows the observed distribution of EGRET blazars. The detection limits of EGRET and GLAST are also shown.

in nice agreement with our model predictions. Therefore we conclude that most of the observed high-energy background radiation from X-ray to 10 GeV spanning 7 orders of magnitude in photon energy can be accounted for by AGNs including blazars, and for the moment we do not have to seriously consider another exotic component of EGRB.

We predicted the flux distribution of blazars by our model, and we found that 400–1500 blazars should be detected by GLAST, assuming a sensitivity of $F_{\rm lim} = 2 \times 10^{-9}$ photons cm^{-2} s^{-1} above 100 MeV. We found that GLAST should resolve almost all of the EGRB flux from blazars, with percentages of $\sim 95\%$ depending on the GLF models. Therefore, we have a clear prediction: if blazars and non-blazar AGNs are the dominant sources of EGRB, the GLAST will resolve almost all EGRB flux into discrete sources at photon energies > 1 GeV, while significant unresolved fraction would remain in the low energy band of < 100 MeV.

References

Aharonian, F. A., Coppi, P. S., & Voelk, H. J. 1994, ApJ, 423, L5

Chiang, J., Fichtel, C. E., von Montigny, C., Nolan, P. L., & Petrosian, V. 1995, ApJ, 452, 156

Chiang, J. & Mukherjee, R. 1998, ApJ, 496, 752

de Boer, W., Sander, C., Zhukov, V., Gladyshev, A. V., & Kazakov, D. I. 2005, A&A, 444, 51

Dermer, C. D. 2007, ApJ, 659, 958

Donato, D., Ghisellini, G., Tagliaferri, G., & Fossati, G. 2001, A&A, 375, 739

Fichtel, C. E., Simpson, G. A., & Thompson, D. J. 1978, ApJ, 222, 833

Fossati, G., Celotti, A., Ghisellini, G., & Maraschi, L. 1997, MNRAS, 289, 136

Fossati, G., Maraschi, L., Celotti, A., Comastri, A., & Ghisellini, G. 1998, MNRAS, 299, 433

Ghisellini, G. & Tavecchio, F. 2008, ArXiv e-prints, 802 Gilli, R., Comastri, A., & Hasinger, G. 2007, A&A, 463, 79

Giommi, P., Colafrancesco, S., Cavazzuti, E., Perri, M., & Pittori, C. 2006, A&A, 445, 843

Gruber, D. E., Matteson, J. L., Peterson, L. E., & Jung, G. V. 1999, ApJ, 520, 124

Hasinger, G., Miya ji, T., & Schmidt, M. 2005, A&A, 441, 417

Inoue, Y., Totani, T., & Ueda, Y. 2008, ApJ, 672, L5

Kamae, T., Abe, T., & Koi, T. 2005, ApJ, 620, 244

Kappadath, S. C., et al. 1996, A&AS, 120, C619+

Keshet, U., Waxman, E., & Loeb, A. 2004, Journal of Cosmology and Astro-Particle Physics, 4, 6

Kneiske, T. M., Bretz, T., Mannheim, K., & Hartmann, D. H. 2004, A&A, 413, 807

Kneiske, T. M. & Mannheim, K. 2008, A&A, 479, 41

Mücke, A. & Pohl, M. 2000, MNRAS, 312, 177

Narumoto, T. & Totani, T. 2006, ApJ, 643, 81

Oda, T., Totani, T., & Nagashima, M. 2005, ApJ, 633, L65

Padovani, P., Ghisellini, G., Fabian, A. C., & Celotti, A. 1993, MNRAS, 260, L21

Padovani, P., Giommi, P., Landt, H., & Perlman, E. S. 2007, ApJ, 662, 182

Pavlidou, V. & Venters, T. M. 2008, ApJ, 673, 114

Pohl, M. & Esposito, J. A. 1998, ApJ, 507, 327

Salamon, M. H. & Stecker, F. W. 1994, ApJ, 430, L21

—. 1998, ApJ, 493, 547

Sazonov, S., Revnivtsev, M., Krivonos, R., Churazov, E., & Sunyaev, R. 2007, A&A, 462, 57

Sreekumar, P., et al. 1998, ApJ, 494, 523

Stecker, F. W., Hunter, S. D., & Kni?en, D. A. 2008, Astroparticle Physics, 29, 25

Stecker, F. W. & Salamon, M. H. 1996, ApJ, 464, 600 Stecker, F. W., Salamon, M. H., & Malkan, M. A. 1993, ApJ, 410, L71

Strong, A. W., Moskalenko, I. V., & Reimer, O. 2004a, ApJ, 613, 956

—. 2004b, ApJ, 613, 962

Thompson, D. J. & Fichtel, C. E. 1982, A&A, 109, 352

Totani, T. & Takeuchi, T. T. 2002, ApJ, 570, 470

Ueda, Y., Akiyama, M., Ohta, K., & Miya ji, T. 2003, ApJ, 598, 886

Watanabe, K., Hartmann, D. H., Leising, M. D., & The, L.-S. 1999, ApJ, 516, 285